Journal of Inorganic Biochemistry 262 (2025) 112749

Contents lists available at ScienceDirect

Journal of Inorganic Biochemistry

journal homepage: www.elsevier.com/locate/jinorgbio

# Pd(II)/1,10-phenanthroline complexes bearing arene ligands: On the role of *N*- vs *O*-coordination to tune their cellular activity and binding ability towards DNA and RNA

Francesca Binacchi [a], Damiano Cirri [a], Eleonora Bimbi [a], Natalia Busto [b,*], Alessandro Pratesi [a,*], Tarita Biver [a,*]

[a] Department of Chemistry and Industrial Chemistry, University of Pisa, Via G. Moruzzi 13, 56124 Pisa, Italy
[b] Departamento de Ciencias de la Salud, Universidad de Burgos, Paseo de los Comendadores s/n, 09001 Burgos, Spain

ARTICLE INFO

*Keywords:*
Metal complexes
Pd(II) cytotoxyc compounds
ROS production
cancer cell selectivity
Coordination
DNA cleavage

ABSTRACT

Three Pd(II)-based complexes of 1,10-phenanthroline and *N*- or *O*-coordinating ligands have been synthesised and tested with different relevant biosubstrates like double-stranded DNA, double and triple helix of RNA, DNA G-quadruplexes of different conformations and bovine serum albumin. Here a correlation between N- vs O-coordinating elements and binding mechanism emerged, where the N-coordinating ligands proved to be the most promising. These outcomes were confirmed also in the cellular experiments. The Pd(II) complex with naphthalene-1,8-diamine is the one that is able to be carried by BSA, to strongly bind nucleic acids, to produce reactive oxygen species (ROS) and to show the best cellular performances (poorly toxic towards healthy cells and highly toxic against the cisplatin-resistant cancer cell line). On the opposite, the complex with benzene-1,2-diolate may be sequestered by BSA, weakly binds nucleic acids, does not produce ROS and shows poor cellular activity. The complex with benzene-1,2-diamine stays in between. Other mechanistic details are discussed which show that the biophysical behaviour is the sum of the contribution of aromaticity, charge and *N*- or *O*-coordination.

## 1. Introduction

The use of platinum complexes as anticancer drugs has been extensively discussed during these years. Cisplatin, carboplatin and oxaliplatin still dominate this field and few new alternatives emerged in the clinical phase. A possible strategy to find new promising drugs was to change the metal centre [1–4]. Palladium(II) complexes are typically an alternative to their platinum(II) counterparts due to the same $d^8$ electronic configuration and coordination geometry, but different chemical properties and biological activity [5]. A recent study that compares Pd(II) and Pt(II) analogues built with quinoline and morpholine ligands revealed that palladium complexes were not only more effective as anticancer but also as antibacterial agents [6]. This property was related to their greater ability to intercalate between DNA base pairs. Indeed, Pd(II) bipyridine species were found to strongly intercalate into DNA; accordingly, they were claimed to be promising candidates for the treatment of leukaemia [7]. Remarkable antitumor properties are also shown by binuclear Pd(II) complexes coordinated by benzothiazoles, which interact thanks to π-π stacking with the nitrogenous DNA bases [8]. On the other hand, the rate of hydrolysis is a critical aspect, given that the ligands leave the Pd(II) metal centre $10^5$ times faster than Pt(II) analogues [5]. This results in the need for very strong (usually nitrogen) ligands and not-labile leaving groups, so to keep the structure intact *in vivo* for the time necessary to reach the anticancer drugs objective [9]. In this frame, the stability in the aqueous solution can be improved also with the use of chelating ligands [10]. Pd(II) complexes bearing 1,10-phenanthroline found application both as catalysts and anticancer drugs [11–14]. The chelating ligand allows stability to the Pd(II) complex, and the extended aromatic planar moiety may lead to intercalating interactions with DNA [10,14–17]. Moreover, the stability and thus the reactivity of Pd(II) complexes are significantly influenced by the ligand environment surrounding the metal centre. It has been demonstrated that the presence of oxygen- or nitrogen-containing bidentate ligands in palladium complexes can affect their stability and reactivity as

* Corresponding authors.
*E-mail addresses:* francesca.binacchi@dcci.unipi.it (F. Binacchi), damiano.cirri@unipi.it (D. Cirri), e.bimbi3@studenti.unipi.it (E. Bimbi), nbusto@ubu.es (N. Busto), alessandro.pratesi@unipi.it (A. Pratesi), tarita.biver@unipi.it (T. Biver).

https://doi.org/10.1016/j.jinorgbio.2024.112749
Received 25 June 2024; Received in revised form 5 September 2024; Accepted 25 September 2024
Available online 28 September 2024

antitumor drugs [18,19]. Oxygen-donating ligands tend to form more stable and less reactive complexes, which can have greater selectivity and lower toxicity but may be less effective at binding to DNA [20]. In contrast, nitrogen-donating ligands form stronger bonds with palladium, creating more reactive complexes that effectively interact with the DNA of cancer cells, although they may also exhibit higher toxicity and lower selectivity [18,21]. The biological effects produced by different coordination elements have been reported also in other systems like in half-sandwich Ir(III) complexes bearing benzazole ancillary ligands. The coordination to CO, N, or $NH_2$ ligands modulates the interaction with DNA or BSA and also the cytotoxic potential [22]. Hence, the electronic and steric effects of these chelate ligands can control the substitution rate and thermodynamic properties of Pd(II) complexes, thereby enhancing their cytotoxic effects against cancer cells by slowing down the kinetics [23,24].

The interest of researchers went also beyond canonical nucleic acids and focused on non-canonical structures of DNA like G-quadruplexes (G4s) [25]. G4s are involved in cell proliferation and are present in telomeres and promoter regions of cancer cells; therefore, G4s became possible drug targets for cancer therapy. Complexes with planar geometries were demonstrated to stabilise these tetrads with stacking interaction above and under the quadruplex structure [25–28]. For instance, some of us found that Pd(II) complexes with quasi-planar aminopyridyl-2,2′-bipyridine tetra dentate ligands stabilise G4s more than their Pt(II) counterpart and interact with RNA four-way junctions [29]. Overall, aromaticity/planarity plays a major role in tuning the reactivity of metal complexes towards G4s; on the other hand, electrostatic aspects are also fundamental, given that oligo and polynucleotides are negatively charged polyelectrolytes [30,31].

In this framework, we propose three new Pd(II) complexes all bearing 1,10-phenanthroline but differentiated by a bidentate aromatic ligand with *N*- or *O*-coordinating groups (Fig. 1). The phenanthroline fosters intercalating/stacking properties, and the other chelating ligand increases the lipophilicity of the compounds with the aim of a higher cellular uptake [14,32]. The different N or *O*-coordinating elements provide the different charges of the complex. This study aims not only at surveying the possible anticancer potency of these still untested Pd(II) complexes but also at analysing their binding mode to evaluate the influence of coordination type, charge, and aromatic extension on their reactivity with different bio substrates.

## 2. Results

### 2.1. Synthesis and stability tests

The synthesis of the title compounds is illustrated in Scheme 1.

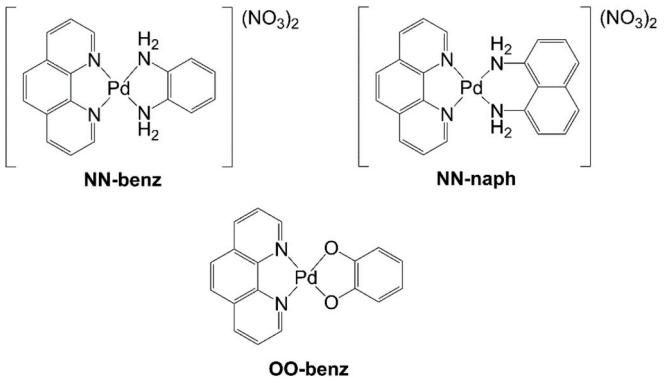


**Fig. 1.** Molecular structures of (1,10-phenanthroline)(benzene-1,2-diamine) palladium(II) dinitrate (NN-benz), (1,10-phenanthroline)(naphthalene-1,8-diamine)palladium(II) dinitrate (NN-naph), (1,10-phenanthroline)(benzene-1,2-diolate)palladium(II) (OO-benz).

First, $PdCl_2$ was solubilized in refluxing acetonitrile to afford to the $[Pd(CH_3CN)_2Cl_2]$ intermediate. The introduction of 1 equivalent of 1,10-phenanthroline leads to a substitution reaction of the two solvent molecules in favour of the bidentate ligand, with the subsequent precipitation of the complex (I) (Fig. S1). Complex (I) was used to obtain the three final compounds. For the *N*-coordinating groups, a first removal of the chloride ligands was necessary, thus an aqueous solution of silver nitrate was added to a solution of (I) in DMF. After the complete formation of AgCl, 1 equivalent of benzene-1,2-diamine or naphthalene-1,8-diamine was added to the mixture in order to obtain compound NN-benz or NN-naph, respectively. After an overnight reaction, the AgCl was filtered off from the solution containing the reaction product, the filtrate was concentrated under vacuum and diethyl ether was added to precipitate the desired Pd complex. To obtain compound OO-benz a simple substitution reaction was performed aided by the addition of KOH to deprotonate benzene-1,2-diolo ligand. The final product was found as a precipitate and recovered through filtration and dried under vacuum. NN-benz, NN-naph, and OO-benz were characterised by $^1H$ NMR (Figs. S2-S4), elemental analysis, and high-resolution mass spectrometry.

Absorbance spectra were recorded with increasing complex concentration (Fig. S5), after 24 h at $T = 25$ °C (Fig. S6), and at different temperatures in buffered solution (NaCl 0.1 mol $dm^{-3}$, NaCac 2.5 mmol $dm^{-3}$, pH = 7.0) (Fig. S7) to verify the linearity of the absorbance in the investigated range and the stability of the obtained Pd complexes. The linearity between absorbance and concentration is respected for all the complexes in the selected concentration ranges (see Fig. S5). The complexes resulted stable over time and the increase in temperature caused very slight changes in the spectral profile of the complexes, except for signal sharpening for NN-naph. Overall, all compounds can be considered stable in the 20–90 °C range; NN-benz and OO-benz do not seem to be prone to undergo significant auto-aggregation, while NN-naph does to some extent, in agreement with its higher aromatic surface. The concentration used in our experiments is around 20 μmol $dm^{-3}$, which is within the range where the aggregation and precipitation phenomena may be supposed to be negligible. Note that higher solubility thresholds may be achieved in the presence of a biosubstrate.

### 2.2. Interaction with DNA and RNA structures

Here below, we first discuss the possible binding towards polynucleotides (natural calf thymus double-strand DNA and double/triple-stranded RNA – from now on denoted as CT-DNA, poly(rA)poly(rU), and poly(rA)2poly(rU)). The absorbance spectra of the three Pd(II) complexes do not allow direct absorbance titration with the nucleic acids, since the profiles do superimpose too much for a precise deconvolution of the absorbance changes. For this reason, melting temperature of metal complex/nucleic acids mixtures, ethidium bromide (EB) exchange tests and viscosity experiments were done. Gel electrophoresis experiments were performed with plasmid DNA (pUC18), alone and in the presence of reactive oxygen species (ROS) scavengers.

#### 2.2.1. Melting

Absorbance spectra of the metal complex/polynucleotide mixtures were recorded at increasing temperatures and plotted at 260 nm (Fig. S8). Solutions of the polynucleotides alone and in the presence of increasing amounts of the Pd(II) complexes were prepared. In the case of CT-DNA, the Pd/DNA ratios $r = 0.4$, 0.6, 0.8, and 1.0 were considered. For RNA, experiments until a Pd/poly(rA)poly(rU) = Pd/poly(rA)2poly (rU) = 1.0 ratio yielded no stabilisation; thus, higher ratios ($r = 1.25$, 1.5 and 2.0) were studied. Fig. 2 collects the results for DNA and poly(rA) poly(rU) (in the case of poly(rA)2poly(rU), $\Delta T_m \approx 0$ in every case).

The results suggest a preference for the DNA double helix structure compared to RNA ones, with a high stabilisation even at low concentrations of the metal complex and NN-naph showing the highest $\Delta T_m$ values. So high differences in the melting temperature (>10 °C) may

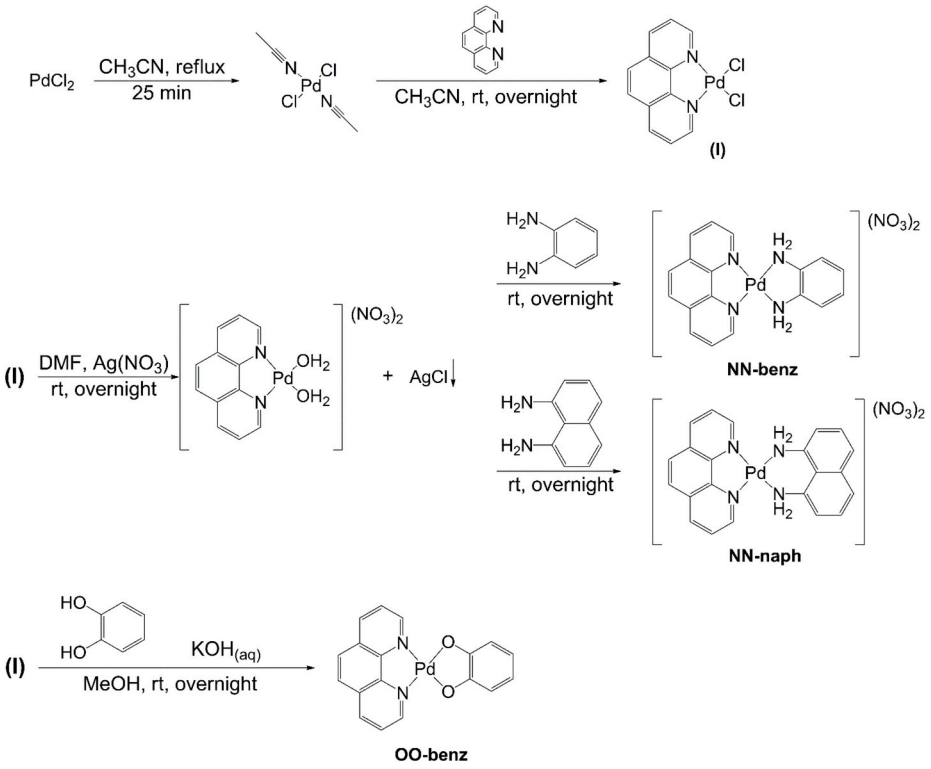


**Scheme 1.** Schematic pathway for the synthesis of NN-benz, NN-naph, OO-benz.

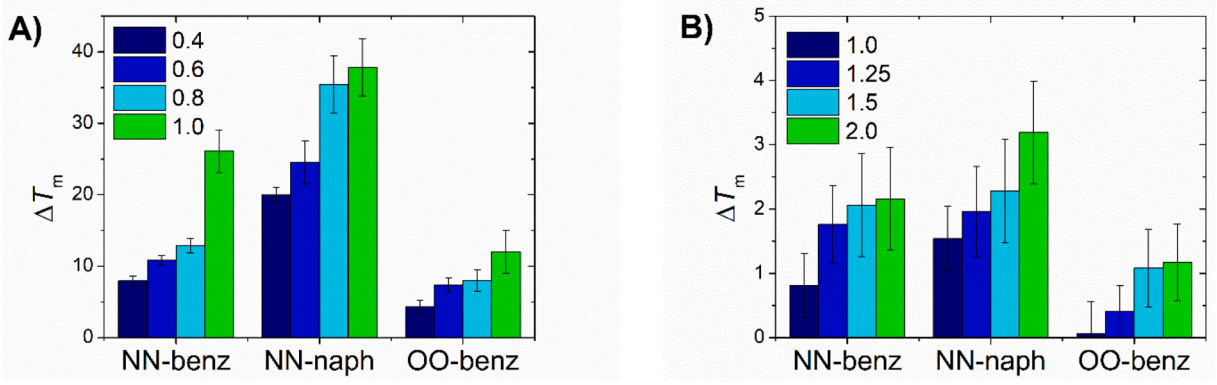


**Fig. 2.** Difference of the melting temperature between the metal complex/nucleotide mixture and the nucleotide alone, $\Delta T_m = T_m$(complex/nucleotide) – $T_m$(nucleotide). (A) For CT-DNA $T_m$ = 54.1 °C, $c_{Pd}/c_{DNA}$ = 0.4, 0.6, 0.8, 1.0; $c_{DNA}$ = 25.5 μmol dm$^{-3}$ in NaCac 2.5 mmol dm$^{-3}$, pH = 7.0. For (B) poly(*rA*)poly(rU) $T_m$ = 56.3 °C, $c_{Pd}/c_{polyAU}$ = 1.0, 1.25, 1.5, 2.0; $c_{polyAU}$ = 14.0 μmol dm$^{-3}$ in NaCl 0.1 mol dm$^{-3}$, NaCac 2.5 mmol dm$^{-3}$, pH = 7.0.

hint for intercalation into the DNA base pairs [33,34]. OO-benz is the less effective in both cases.

### 2.2.2. *Ethidium bromide exchange*

Ethidium bromide (EB) is used to perform exchange experiments where a solution of CT-DNA, poly(rA)poly(rU), or poly(rA)2poly(rU) saturated with EB is retro-titrated with the metal complex. Note that the metal complex solutions contain a certain percentage of DMSO. Therefore, a negative control experiment was performed by adding the same amount of DMSO: no significant signal changes were detected. Conversely, all NN-benz, NN-naph and OO-benz were able to displace EB from its intercalation pocket: Fig. 3 shows the decrease in the fluorescence of the EB/polynucleotide adduct as a function of r = $c_{Pd}$/$c_{polynucleotide}$.

Some preference for CT-DNA is confirmed (higher plot curvatures and fluorescence decrease), and the displacement efficiency always follows the order NN-naph > NN-benz > OO-benz. OO-benz results as less effective at lower ratios (for instance r= 1.0, in agreement with the melting experiments) but, when an excess of the metal complex is added, also this compound can produce effects comparable to the other two Pd complexes. For the triplex structure, NN-benz and OO-benz are much less effective. These results suggest a strong interaction of the metal complexes with the polynucleotides, higher in the case of NN-naph. A contribution from the groove can be speculated, in particular for NN-benz and OO-benz. Indeed, the results of the test change for the RNA triplex, where the polyU filament occupies the polyAU groove. On the other hand, groove binding needs to be particularly effective to produce such a great intercalated EB displacement ability. On the whole, it seems that an intricate binding mode is the most likely picture. Intercalation or groove binding may differently contribute to the overall binding mode, as a function of the type of both metal complex and polynucleotide. Other tests were done to get additional information (see below).

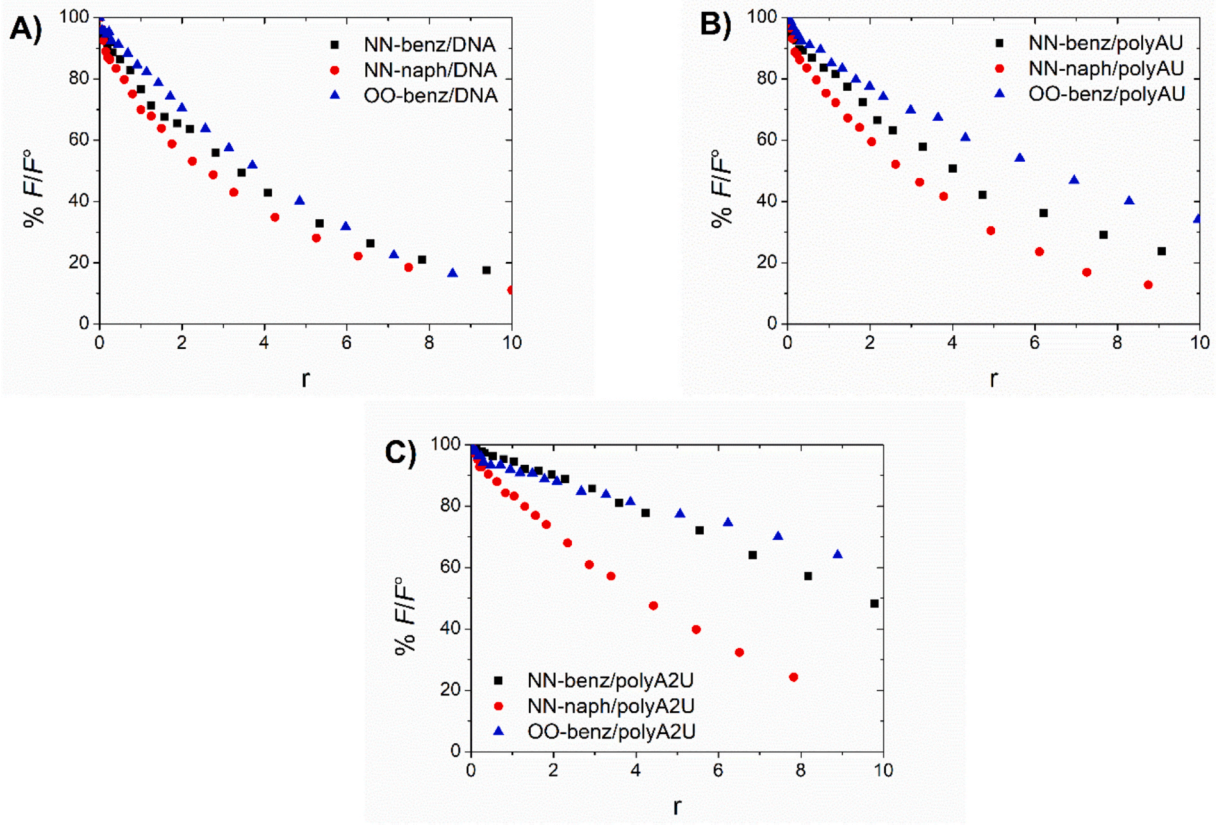


**Fig. 3.** EB exchange tests where the metal complexes are added to EB-saturated (A) CT-DNA, (B) poly(rA)poly(rU), and (C) poly(rA)2poly(rU) solutions. The EB/polynucleotide adduct is strongly fluorescent only when the EB probe is intercalated between the polynucleotide base pairs; (A) $c_{DNA} = 27.5$ μmol dm$^{-3}$, $c_{EB} = 12.3$ μmol dm$^{-3}$; (B) $c_{polyAU} = 23.3$ μmol dm$^{-3}$, $c_{EB} = 11.6$ μmol dm$^{-3}$; (C) $c_{polyA2U} = 25.5$ μmol dm$^{-3}$, $c_{EB} = 11.4$ μmol dm$^{-3}$; r = $c_{Pd}/c_{polynucleotide}$, relative fluorescence = 100*F/F° where F° is the fluorescence of the system at $r = 0$, $\lambda_{ex} = 520$ nm, $\lambda_{em} = 595$ nm. NaCl 0.1 mol dm$^{-3}$, NaCac 2.5 mmol dm$^{-3}$, pH = 7.0, $T = 25.0$ °C.

### 2.2.3. Viscosity

The viscometric analysis was carried out by keeping the DNA concentration constant ($c_{DNA} = 118$ μmol dm$^{-3}$) and varying the metal concentration of the complex to obtain $c_{Pd}/c_{DNA}$ from 0 to 1.0. Fig. S9 shows the cubic root of the relative viscosity of $\eta/\eta^{\circ}$, as a function of r = $c_{Pd}/c_{DNA}$.

There is a substantial constancy of the relative viscosity for NN-naph, whereas a slight decrease for the NN-benz and OO-benz compounds. The discussion on this behaviour is not straightforward, given that many aspects contribute to change the hydrodynamic response of polynucleotides. Classical intercalation typically involves elongation and, consequently, an increase in viscosity [35]. However, the effect would be milder for partial intercalation, or even turn into compaction (viscosity decrease) if the helix bends over a semi-intercalated form [36]. The covalent binding of the metal centre decreases the viscosity [37]. High thermal stabilisation and a decrease in the duplex length have been previously described in complexes with dual activity: intercalation of the ancillary ligand and coordination to the metal centre [38]. What can undoubtedly be said here is that NN-benz and OO-benz behave the same way, whereas NN-naph does something different/more.

### 2.2.4. Gel electrophoresis

The interaction of the three Pd(II) complexes with DNA was further investigated with agarose gel electrophoresis with pUC18. Solutions of DNA alone and with an increasing amount of complexes NN-benz and NN-naph were studied at no incubation time and after 24 h of incubation (Fig. 4). With no incubation time, a decrease in the migration rate of the supercoiled circular (SC) lane is observed as the concentration of NN-benz and NN-naph is increased. This behaviour correlates well with the intercalation of the complexes between the DNA base pairs [39] and

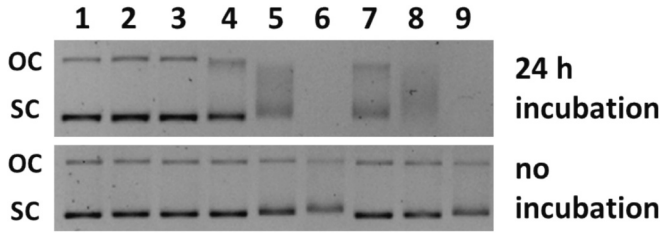


**Fig. 4.** Electrophoresis mobility assay at 24 h of incubation time and no incubation of 1) pUC18 (6.5 μmol dm$^{-3}$) with: 2) max % of DMSO; 3–6) NN-benz in a ratio $c_{Pd}/c_{pUC18} = 0.1, 0.5, 1, 3$; 7–9) NN-naph in a ratio $c_{Pd}/c_{pUC18} = 0.1, 0.5, 1$. NaCac 2.5 mmol dm$^{-3}$, pH = 7.0.

is not shown in the case of OO-benz. By contrast, after 24 h of incubation, DNA cleavage is observed, and the disappearance of the plasmid lanes is observed at a concentration ratio of Pd/pUC18 = 3 and 1, respectively, for NN-benz and NN-naph. Complex OO-benz is not able to induce any conformational change of the plasmid after 24 h even at higher ratios (Fig. S10). To assess the cleavage, an experiment with the NN-benz/pUC18 system over time was performed by freezing aliquots of 1:1 mixture from 0 h to 24 h of incubation: Fig. S11 shows the formation of the linear strand of DNA which runs between the OC (open circular) and SC conformations. Moreover, the linear strands tend to disappear over time till a complete fragmentation in 24 h. This is in agreement with the previous experiments, where a high stabilisation and displacement of EB were noticed. The ability of Pd(II) complexes to cleave DNA was extensively described [8,40]. However different mechanisms were proposed, a hydrolytic pathway was hypothesized for Pd(II) saccharinate complexes with terpyridine [41] whereas an

oxidative mechanism was confirmed for other Pd(II) complexes [42,43]. To elucidate the possible mechanism for the observed DNA damage and considering that the bleaching of the bands with the loss of the total presence of plasmid signal (Fig. 4) could be caused by reactive oxygen species (ROS), which produced an extreme cleavage of DNA up to small strands, another electrophoresis experiment was performed in presence of an excess of ROS scavengers (Fig. 5). The conditions chosen are $c_{Pd}/c_{pUC18} = 3$ for NN-benz and $c_{Pd}/c_{pUC18} = 1$ for NN-naph, i.e. where the cleavage started to be evident.

For both NN-benz and NN-naph complexes, there is no more DNA cleavage in the presence of SOD and L-His. These ROS scavengers are respectively focused on $^1O_2$, and $O_2^-$ [39]. Therefore, it is demonstrated that these two compounds, once bound to DNA, produce ROS, and cleave the DNA strands.

On the whole, these results suggest that a slow reaction is at work and that the interaction mechanism is influenced by the different coordinating atoms, *N* vs *O*. A mixed mode (partial intercalation/groove) is the binding mode in short-time experiments (titrations, melting and viscosity). The metal complex NN-naph is, under these circumstances, the more efficient (more extended planar part), together with NN-benz (they are both positively charged species). Electrophoresis data at $t = 0$ confirm their intercalation already in short time ranges. Intercalation and groove binding are non-covalent binding modes known to be fast reactions, occurring in the sub-second time range [44]. On the other hand, some additional reaction occurs in long-time spams for NN-benz and NN-naph. In agreement with such slow kinetics, it may be speculated that, in the case of the more labile Pd-$NH_2$ coordination, covalent binding of the Pd metal centre to the DNA bases occurs as one of the Pd-$NH_2$ bonds is broken and there is the production of ROS. All of this does not occur in the case of OO-benz. Due to the stronger coordination to oxygen and neutral charge, is not only less prone to bind DNAs and RNAs at fast time ranges but cannot produce either cleavage or ROS formation over slower time spams. This picture would agree with the work of Anbalagan and Srivastava [45] who found a significant $^1O_2$ generation in complexes bearing α-diimine ligands, with an efficacy that depends on the number of condensed aromatic rings.

### 2.3. Interaction with G-quadruplex

The metal complexes NN-benz, NN-naph, and OO-benz were tested also with three G-quadruplex (G4) conformations by measuring the melting temperature in the absence and presence of the metal complexes at a 1:1 ratio with the G4. Fig. S12 shows the data obtained as a function of temperature, and Fig. 6 collects the $\Delta T_m$. None of the three complexes shows significant stabilisation/destabilisation of the hybrid Tel-23 or parallel c-myc structures: the $|\Delta T_m|$ are negligible being <2 °C. The antiparallel CTA-22 conformation is the one that undergoes some effect, and is stabilised by NN-benz, NN-naph, and OO-benz. The most significant outcome is the stabilisation of CTA-22 ($\Delta T_m = 5.0 \pm 0.6$ °C) produced by NN-naph. In this case, the extended aromaticity of the complex may have favoured stacking interaction with the guanine quartets.

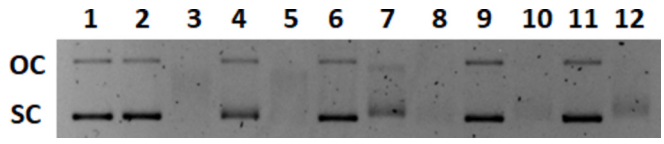


**Fig. 5.** Electrophoresis mobility assay: 1) pUC18 (6.5 μmol $dm^{-3}$), 2) with max % of DMSO; 3 and 8) with NN-benz and NN-naph in a ratio $c_{Pd}/c_{pUC18} = 3.0$ and 1.0 respectively. Complexes in the presence of ROS scavengers: 4 and 9) SOD (4000 U $cm^{-3}$); 5 and 10) pyr (1 mmol $dm^{-3}$); 6 and 11) L-Hist (1.2 mmol $dm^{-3}$); 7 and 12) DMSO (200 mmol $dm^{-3}$). Buffer: NaCac 2.5 mmol $dm^{-3}$, pH = 7.0.

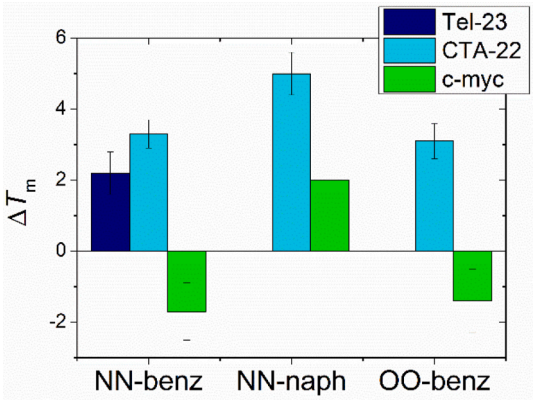


**Fig. 6.** Difference of the melting temperature between the metal complex/G4 mixture and the G4 alone, $\Delta T_m = T_m$(complex/G4) – $T_m$(G4). $T_m$(Tel-23) = 62.8 °C, $T_m$(CTA-22) = 62.6 °C, $T_m$(c-myc) = 73.9 °C. $c_{Pd}/c_{G4} = 1.0$ where $c_{CQ}$ = 25.5 μmol $dm^{-3}$. KCl 0.1 mol $dm^{-3}$, LiCac 2.5 mmol $dm^{-3}$, pH 7.0 for Tel23 and CTA22; KCl 0.01 mol $dm^{-3}$, LiCac 2.5 mmol $dm^{-3}$, pH 7.0 for c-myc.

### 2.4. Interaction with BSA

#### 2.4.1. Titrations

The interaction of the Pd(II) complexes with the BSA protein was studied by spectrofluorimetric titrations. The three Pd(II) complexes do not emit light in these conditions. The titrations were performed in 0.1 mol $dm^{-3}$ NaCl, 2.5 mmol $dm^{-3}$ NaCac, pH = 7.0 buffer, at 25.0, 37.0 and 45.0 °C (triplicates). As an example, the titrations at 25.0 °C are reported (Fig. S13). Equilibrium constants were calculated with the modified Stern Volmer equation (Table S1) and Scatchard equation (Table S2) to verify the static quenching of BSA, formation of an adduct with Pd complexes, and the reaction stoichiometry respectively. The high Stern-Volmer constants confirmed the effective interaction between Pd complexes and BSA, while from the Scatchard equation a 1:1 binding mode was assessed. On this basis, the HypSpec® software was used with a 1:1 binding model for the calculation of the equilibrium constants. The latter are resumed in Table S2. Ultimately, these data show that all three complexes of Pd(II) interact with the BSA with equilibrium constants of the magnitude order of $10^5$ –$10^6$ i.e. in the typical window that allows the transport in biological fluids, with no selectivity. Within the errors, the equilibrium constants do not significantly depend on temperature, in agreement with a $\Delta H \approx 0$ process. This latter result indicates a weak reversible interaction of the small molecules with BSA pockets in the fast time scales.

#### 2.4.2. Native gel electrophoresis

During the spectrofluorimetric titrations (done within 3 h), no differences were observed between the three compounds. The interaction with the protein was deepened by evaluating possible conformational changes after long incubation times (24 h). In this context, native gel electrophoresis tests were performed. This technique can detect possible conformational changes of the protein upon interaction with the metal complexes, revealed by the appearance of new bands during the electrophoresis run. Solutions of BSA alone and in the presence of increasing amounts of the metal complexes ($c_{Pd}/c_{BSA} = 5.0$, 10 and 20) were prepared and incubated for 24 h at 37.0 °C. Then, the solutions were loaded into the gel and the run was performed at 4 °C to avoid any possible denaturation of the protein. NN-benz and OO-benz produced a new BSA band starting from a ratio of 10:1 (Pd:BSA), while NN-naph did not produce any conformational change (Fig. 7). A negative control with DMSO alone was done, confirming no denaturation process caused by DMSO.

This behaviour suggests that 24 h incubation allowed NN-benz and OO-benz to exert a more complex binding mechanism. The presence of significant BSA conformational changes after 24 h incubation with NN-

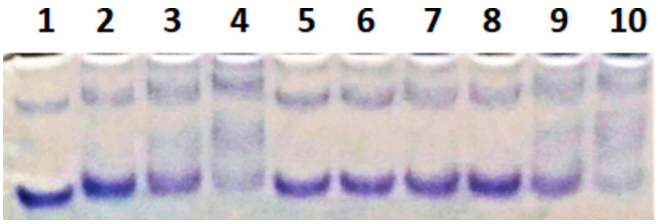


**Fig. 7.** Native acrylamide electrophoresis of BSA (2 μmol $dm^{-3}$) incubated for 24 h with NN-benz, NN-naph and OO-benz. 1) BSA with 0.78 % of DMSO. 2–4) with NN-benz in a ratio $c_{Pd}/c_{BSA}$ = 5.0, 10, and 20; 5–7) with NN-naph in a ratio $c_{Pd}/c_{BSA}$ = 5.0, 10, and 20; 8–10) with OO-benz in a ratio $c_{Pd}/c_{BSA}$ = 5.0, 10, and 20. Final max DMSO concentration = 0.78 %. Buffer: NaCl 0.1 mol $dm^{-3}$, NaCac 2.5 mmol $dm^{-3}$, pH = 7.0.

benz or OO-benz indicates a strong/covalent binding which turns into sequestration of the metal complexes by the protein [46]. These conformational changes are not observed in the case of NN-naph, whose action is limited to the $\Delta H \approx 0$ process seen in direct fluorescence titrations (fast time scales). On this basis, we may infer that NN-naph only non-covalently/reversibly binds BSA

### 2.5. Biological studies

#### 2.5.1. Antiproliferative activity

To evaluate the antiproliferative activity of complexes NN-benz, NN-naph, and OO-benz, four cancer and one normal cell lines were selected. A549 (lung cancer), SW480 (colon cancer), A2780 (ovarian cancer), A2780cis (ovarian cancer resistant to cisplatin) and HEK293 (human embryonic kidney) were incubated with increasing amounts of the complexes for 24 h. MTT test was used to evaluate the $IC_{50}$ values listed in Table 1 and compared to that of cisplatin (CDDP). The antiproliferative activity is dependent on the cell type. For the A549 cell line, the cytotoxicity was comparable to CDDP, while for SW480, NN-naph and OO-benz were the most cytotoxic. All Pd complexes display higher cytotoxic potential in A2780cis with respect to cisplatin. Interestingly, compound NN-naph was the most promising with an $IC_{50}$ value of 3 and 4 μmol $dm^{-3}$ in A2780 and A2780cis, respectively. These $IC_{50}$ values suggest that this complex could be able to overcome the cisplatin resistance in the A2780 cancer cell line. Importantly, NN-benz and NN-naph were less toxic for the healthy cell line HEK293, and NN-naph was the one with the highest selectivity index (SI = 12). Overall, complex NN-naph showed a better profile both for resistance factor and selectivity properties.

#### 2.5.2. Flow cytometry

To assess if the death mechanism is apoptotic or necrotic, a flow cytometry experiment was performed. Annexin V-FITC/PI double staining test was used on SW480 cells. The sum of cells in early and late apoptosis was higher compared to the number of cells in necrosis for all the complexes (Fig. 8). These values confirm that the cell death mechanism is apoptosis, compatible with the DNA damage pathway.

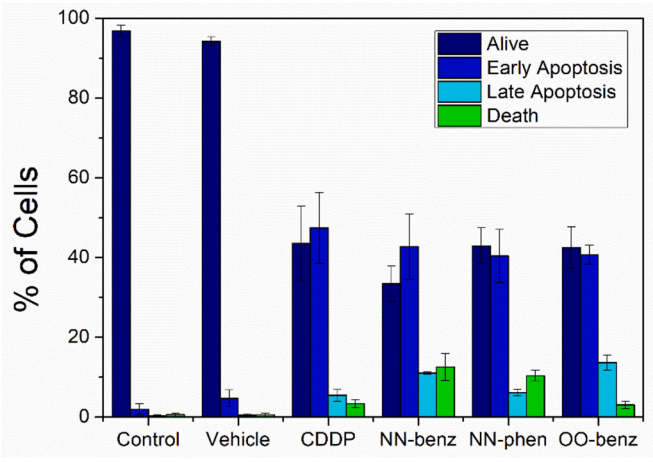


**Fig. 8.** Flow cytometry of human colon carcinoma cells (SW480) after 24 h of incubation, treated at the $IC_{50}$ concentration of the complex.

#### 2.5.3. Cellular uptake

The cellular uptake was performed on the SW480 cancer cell line and the values are reported as μmol of metal divided by the total number of cells (Table 2). Cisplatin was used as a reference, with the corresponding values of the lipophilicity of the complexes expressed as the logarithm of the partition coefficient between octanol and water phases ($logP_{o/w}$). The charged compounds, NN-benz and NN-naph, are the most internalised and have higher values compared to cisplatin, while the neutral compound OO-benz is less: internalisation follows the order NN-benz > NN-naph > OO-benz. Here, the internalisation of the three Pd(II) complexes is conversely correlated to the degree of lipophilicity: for $logP_{o/w}$ OO-benz > NN-naph ≈ NN-benz. These orders do not correlate much with that of cytotoxicity (for SW480, NN-naph ≈ OO-benz > NN-benz). This means that additional factors are at play, such as the complexes not being equally distributed in different cellular compartments.

The antiproliferative outcomes can now be discussed on the basis of the mechanistic properties of biosubstrates interaction shown above. Complex NN-naph is able to intercalate into DNA, produces ROS at lower concentrations compared to NN-benz, stabilises antiparallel G4, and reversibly binds BSA, according to a mode which allows the release of the complex to the cells. This complex showed high uptake inside the cells, likely due to a better balance of protein delivery and lipophilicity ($logP_{o/w}$). All these properties may explain the lower $IC_{50}$ values. Complex OO-benz is the one which showed the less interesting profile. It emerged as a groove binder for polynucleotides, not stabilising the structures as efficiently as the other complexes. OO-benz is probably partially sequestrated by proteins, which may explain the lower uptake values. Moreover, it is the only one which cannot cleave DNA and turned out completely unselective for cancer cells. Complex NN-benz showed a mean behaviour compared to the other two complexes.

## 3. Conclusion

Three new Pd(II) complexes bearing 1,10-phenanthroline and arene ligands with N or O coordinating groups were synthesised and

**Table 1**
$IC_{50}$ values (μmol $dm^{-3}$) after 24 h of incubation, mean ± SD from 3 independent experiments.

| | A549 | SW480 | A2780 | A2780cis | RF[a] | HEK293 | SI [b] |
|---|---|---|---|---|---|---|---|
| **NN-benz** | 39 ± 5 | 42 ± 5 | 16 ± 2 | 14 ± 1 | 1 | 50 ± 10 | 3 |
| **NN-naph** | 56 ± 10 | 14 ± 2 | 4 ± 1 | 3 ± 1 | 1 | 47 ± 6 | 12 |
| **OO-benz** | 39 ± 7 | 18 ± 3 | 11 ± 1 | 20 ± 3 | 2 | 15 ± 2 | 1 |
| **CDDP** | 39 ± 2 | 35 ± 2 | 8 ± 1 | 30 ± 3 | 4 | 15 ± 2 | 2 |

[a] RF (resistance factor) = $IC_{50,A2780cis}$ / $IC_{50,A2780}$.
[b] SI (selectivity index) = $IC_{50,HEK293}$ / $IC_{50,A2780}$.

**Table 2**
Cellular uptake expressed as μmol of metal (M) in the total number of counted cells, after 24 h of incubation at 37 °C. $logP_{o/w} = log([complex]_o / [complex]_w)$.

| | μmol M/cells ($10^{-7}$) (M = Pd, or Pt) | $logP_{o/w}$ |
|---|---|---|
| **NN-benz** | 6.8 ± 0.5 | −1.3 |
| **NN-naph** | 5.6 ± 0.5 | −1.4 |
| **OO-benz** | 3.0 ± 0.2 | 0.2 |
| **CDDP** | 3.8 ± 0.5 | −2.4 |

characterised. Complex NN-naph (positively charged, higher aromaticity) was demonstrated to strongly interact with both DNA and RNA polynucleotides, with evidence for an intercalative interaction. NN-naph is also the one that stabilised most DNA G4, with selectivity for CTA-22 (antiparallel). On the other hand, the observed binding of NN-naph with the BSA protein is related to weak forces enabling delivery and release to the cells. Also, NN-naph is very selective for cancer cells and overcomes cisplatin resistance in A2780cis. OO-benz is the least reactive and managed to stabilise efficiently only DNA. On the other hand, for BSA, OO-benz binds so tightly to the protein (producing significant conformational changes after incubation) that it may likely be sequestered. Importantly, after 24 h incubation, NN-benz and NN-naph produce DNA cleavage by an oxidative mechanism involving ROS generation. This could be a possible mechanism of action for cell death, which differs from the one of cisplatin and which would be linked to the presence of *N*-coordination. On the whole, the biological profiles of the studied metal complexes were found to be related not only to some non-covalent fast-time scale binding but to the presence of slow effects strongly influenced by the coordination type. The Pd(II) complexes with *N*-coordination are here the ones with better reactivity. Further studies are being planned to enlarge the panel and better describe the slow effects and the geometries of the final adducts.

## 4. Experimental section

### 4.1. Materials

All the materials for the synthesis were purchased from Merck or Fluorochem. The deuterated solvents were purchased from Deutero.

Metal complex stock solutions were prepared by dissolving a known weighted amount of the compound (≈ 2 mg) in dimethylsulfoxide (DMSO) to obtain a final solution concentration of 2–20 mmol $dm^{-3}$.

Calf thymus DNA (CT-DNA), natural DNA from calf thymus, lyophilised sodium salt from Sigma-Aldrich (double strand in the B-helix form when in the buffer) was dissolved in ultrapure water and previously sonicated to have about 500 base pairs. Its concentration in the stock was about 2.5 mmol $dm^{-3}$ expressed in base pairs. Before its use, the exact concentration value was checked by acquiring an absorption spectrum. The absorption peak considered is $\lambda = 260$ nm and the $\varepsilon$ at that wavelength is equal to 13,200 $cm^{-1}$ $mol^{-1}$ $dm^3$ [47]. In this way, a molar concentration of DNA in base pairs ($c_{DNA}$) was obtained. Natural DNA of the plasmid, pUC18 (2686 base pairs in length) was extracted from *E. coli* DH5α. The DNA G-quadruplexes (G4) used were formed by different telomeres to have different types of conformations: 5′-TAGGGTTAGGGTTAGGGTTAGGG-3′ (Tel-23 – hybrid); 5′-AGGGCTAGGGCTAGGGCTAGGG-3′ (CTA-22 – antiparallel); 5′-TGAGGGTGGGTAGGGTGGGTAA-3′ (c-myc – parallel) were dissolved in KCl 0.1 mmol $dm^{-3}$, LiCac 2.5 mmol $dm^{-3}$, pH = 7.0 obtaining a solution of G4 ($c_{G4}$) 1 mmol $dm^{-3}$. For the annealing procedure, a literature procedure was followed [48]. Poly(rA) and poly(rU) were purchased by Sigma-Aldrich as model polynucleotides of RNA structures. Poly(rA) was used as a single filament in NaCl 0.1 M, NaCac 2.5 mM pH = 7.0 buffer, whose concentration was measured by spectrophotometry considering the peak at 257 nm ($\varepsilon$ = 10,110 $cm^{-1}$ $mol^{-1}$ $dm^3$) [49] obtaining a concentration expressed as phosphate groups ($c_A$) of 8.4 mmol $dm^{-3}$. For the double helix, a poly(rU) solution was prepared in the same buffer whose concentration was measured considering the peak at 260 nm ($\varepsilon$ = 8900 $cm^{-1}$ $mol^{-1}$ $dm^3$) [49] obtaining a concentration value of 14 mmol $dm^{-3}$. A solution of poly(rA) with poly(rU) in a 1:1 ratio in buffer was then prepared and left to stand overnight in the dark at room temperature to obtain the double helix poly(rA)poly(rU) concentration in base pairs ($c_{AU}$) 2.0 mmol $dm^{-3}$ [50]. For the triple helix, a solution was prepared by combining poly(rA)·poly(rU) with poly(rU) in a 1:1 ratio in buffer and left to stand overnight at room temperature to allow the integration of a third filament in the structure, thus obtaining a solution of poly(rA)2poly(rU) of concentration in base triplet ($c_{A2U}$) 0.4 mmol $dm^{-3}$ [51].

The BSA solution was prepared by weighing freeze-dried BSA (lyophilized powder, essentially fatty acid free, ≥98 % (agarose gel electrophoresis) purchased from Sigma-Aldrich (MW ≈ 66 kDa) by dissolving it in NaCl 0.1 mol $dm^{-3}$, NaCac 2.5 mmol $dm^{-3}$, pH = 7.0 buffer. The effective concentration was determined by spectrophotometry considering the absorption at 278 nm ($\varepsilon$ = 45,000 $cm^{-1}$ $mol^{-1}$ $dm^3$) [52] obtaining a solution of BSA ($c_{BSA}$) 80.0 μmol $dm^{-3}$.

The used buffer solutions were prepared by dissolving a known amount of the desired salts in MilliQ water, obtained through an "AriumPro SARTORIUS" device, and the pH was checked by a previously calibrated pH-meter. The pH was possibly corrected by making micro additions of HCl or concentrated NaOH. Working solutions for the analyses are obtained by dilution of the metal complex or biosubstrates in the correct buffer. In these working solutions, the dilution with the aqueous buffer is such that DMSO content can be considered negligible (<1 %).

### 4.2. Synthesis

#### 4.2.1. Synthesis of the intermediate (I), [$PdCl_2$(phen)]

The intermediate [$PdCl_2$(phen)] (phen = 1,10-phenanthroline) was prepared in a two-step reaction. First, 0.695 g of $PdCl_2$ (3.92 mmol) were weighed and suspended in 20 $cm^3$ of acetonitrile. The suspension was refluxed until complete $PdCl_2$ dissolution. After 25 min, the solution was clear, indicating that [$Pd(CH_3CN)_2Cl_2$] was formed. Secondly, heating was stopped and solid phenanthroline (1 eq.) (0.710 g, 3.94 mmol) was added to the reaction round flask. The formation of a precipitate was immediately observable. The reaction was kept under stirring at room temperature, overnight. The following day, the mixture present in the flask was filtered, and the solid product was washed with diluted hydrochloric acid, diethyl ether and dried under vacuum, affording 1.34 g (3.75 mmol) of the pure product (yield 96 %).

$^1$H NMR (DMSO-$d_6$, 400.13 MHz, 298 K): $\delta$ = 9.66 (d, 2H), 9.00 (d, 2H), 8.26 (s, 2H), 8.13 (t, 2H) ppm; (Fig. S1).

#### 4.2.2. Synthesis of NN-benz

The complex (1,10-phenanthroline)(benzene-1,2-diamine)palladium(II) dinitrate, here called NN-benz, was prepared in a two-step reaction. First, 0.088 g (0.25 mmol) of [$PdCl_2$(phen)] were weighed and solubilized in 2.5 $cm^3$ of DMF in a 50 $cm^3$ round flask. Separately an aqueous solution of $AgNO_3$ (0.084 g, 0.49 mmol) in 1.5 $cm^3$ of distilled water was prepared and added to the mixture in the reaction flask. The reaction was performed at room temperature, overnight. The addition of the aqueous solution of silver nitrate is done to promote the detachment of the chloride ligands through the precipitation of AgCl, and thus to activate the Pd(II) intermediate forming [$Pd(H_2O)_2$(phen)]$(NO_3)_2$, that is the reactive specie for the subsequent binding to benzene-1,2-diamine.

The following day, 0.0266 g (0.246 mmol) of benzene-1,2-diamine solubilized in 1 $cm^3$ of DMF was added in 1:1 stoichiometry with [$Pd(H_2O)_2$(phen)]$(NO_3)_2$ to the reaction mixture. The reaction was performed overnight at room temperature. The following day the reaction was stopped, and the suspension was filtered through celite to remove AgCl. The filtrate was recovered and pre-concentrated in the rotavapor ($T$ of the water bath = 37 °C). Once a few $cm^3$ of DMF were removed, diethyl ether was added to favour the precipitation of the complex. The precipitate was filtered, and the recovered solid product was washed on the filter with diethyl ether and dried. 0.1277 g (0.2461 mmol) of NN-benz (yield 98 %).

$^1$H NMR (MeOH-d4, 400.13 MHz, 298 K): $\delta$ = 9.05 (dd, 2H), 8.95 (dd, 2H), 8.32 (s, 2H), 8.20 (d, 1H), 8.19 (d, 1H), 7.54 (m, 2H), 7.47 (m, 2H) ppm (Fig. S2).

Elemental analysis calc (%) for $C_{18}H_{16}N_6O_6Pd$: C 41.67, H 3.11, N 16.20; found (%) C 41.69, H 3.09, N 16.17.

ESI-TOF-MS: ion type = $[M]^{2+}$, $m/z$ found = 196.01153, $m/z$ calc =

196.01211.

#### 4.2.3. Synthesis of NN-naph

The complex (1,10-phenanthroline)(1,8-diaminonaphtalene)palladium(II) dinitrate, here called NN-naph, was prepared in a two-step reaction similarly to NN-benz. First, 0.051 g (0.14 mmol) of $[PdCl_2(phen)]$ were weighed and solubilized in 2 $cm^3$ of DMF in a 50 $cm^3$ round-bottom flask. Separately an aqueous solution of $AgNO_3$ (0.048 g, 0.28 mmol) in 1 $cm^3$ of bi-distilled water was prepared and added to the mixture in the reaction flask. The reaction was performed at room temperature, overnight, to form $[Pd(H_2O)_2(phen)](NO_3)_2$.

The following day, 0.0225 g (0.142 mmol) of naphthalene-1,8-diamine solubilized in 1 $cm^3$ of DMF was added in a 1:1 stoichiometry with $[Pd(H_2O)_2(phen)](NO_3)_2$ to the reaction mixture. The reaction was performed at room temperature, overnight. Hence, the obtained suspension was filtered through celite to remove the formed AgCl. The filtrate was recovered and pre-concentrated in the rotavapor ($T$ of the water bath = 37 °C). Once a few $cm^3$ of DMF were removed, diethyl ether was added to favour the precipitation of the complex. The precipitate was filtered and the solid was washed on the filter with diethyl ether. Subsequently, the product was dried under vacuum, and 0.0606 g (0.106 mmol) of NN-naph (yield 76 %).

$^1$H NMR (MeOH-d4, 400.13 MHz, 298 K): $\delta$ = 9.40 (dd, 2H), 9.29 (dd, 2H), 8.98 (dd, 2H), 8.87 (dd, 2H), 8.24 (s, 2H), 7.67 (m, 2H), 7.55 (m, 2H) ppm (Fig. S3).

Elemental analysis calc (%) for $C_{22}H_{18}N_6O_6Pd$: C 46.45, H 3.19, N 14.77; found (%) C 46.48, H 3.12, N 14.73.

ESI-TOF-MS: ion type = $[M]^{2+}$, $m/z$ found = 222.02666, $m/z$ calc = 222.02776.

#### 4.2.4. Synthesis of OO-benz

The complex (1,10-phenanthroline)(benzene-1,2-diolate)palladium (II), here called OO-benz, was prepared in a two-step reaction. First 0.401 g of $[PdCl_2(phen)]$ (1.12 mmol) and 0.123 g of benzene-1,2-diolo (1.12 mmol) were weighted and suspended in 15 $cm^3$ of methanol. Separately, an aqueous solution containing 2 equivalents of KOH (0.126 g, 2.25 mmol) was prepared and added to the reaction mixture. KOH solution was used to deprotonate benzene-1,2-diolo ligand and promote the binding to the metal centre. A rapid change in the colour of the mixture (from yellow to brick red) was immediately noticed. The reaction was performed at room temperature, overnight. The following day, the brick red solid precipitate was filtered and washed with diethyl ether (20 $cm^3$). Subsequently, the product was dried under vacuum, and 0.2714 g (0.6876 mmol) of pure OO-benz (yield 61 %) were recovered.

$^1$H NMR (MeOH-d4, 400.13 MHz, 298 K): $\delta$ = 8.86 (dd, 2H), 8.76 (dd, 2H), 8.13 (s, 2H), 7.99 (d, 2H), 7.97 (d, 2H), 6.52 (m, 2H), 6.40 (m, 2H) ppm (Fig. S4).

Elemental analysis calc (%) for $C_{18}H_{12}N_2O_2Pd$: C 54.77, H 3.06, N 7.10; found (%) C 54.25, H 3.01, N 7.07.

### 4.3. Methods

#### 4.3.1. Spectrophotometry and spectrofluorometry

A *Shimadzu UV-2450* or a *Perkin Elmer Lambda 35* double-beam UV–vis spectrophotometer were used for absorbance experiments. Both instruments are equipped with a tungsten lamp for visible light and a deuterium lamp for the UV range. The fluorescence data were recorded with an *LS55 Perkin-Elmer* spectrofluorometer. The excitation light is provided by a pulsed Xenon lamp (50 Hz). All the instruments have jacketed cell holders providing temperature control within ±0.1 °C. All spectra were recorded using quartz cuvettes of 1 $cm^3$ or 0.5 $cm^3$ minimum volume and an optical path of 1.0 cm. Fluorescence experiment conditions were carefully chosen (high dilution, wavelengths) and checked so to ensure direct proportionality between reading and fluorophore concentration.

#### 4.3.2. Melting experiments

Melting experiments were performed following the absorbance changes (260 nm for CT-DNA and RNA, 290 nm for G4s) at increasing temperatures ranging from 25.0 °C to 90.0 °C. The scan rate is +5.0 °C/min every 7.5 min, and the solution stays at the current temperature for 5 min before the spectrum is recorded (1.5 min for the recording). To reach the following temperature 1 min is needed. Cuvettes of 1.0 cm, 2.0 mm or 1.0 mm light path were used depending on the experiment. The short light path was needed for the oligos (DNA G4s) melting tests.

The percentage of absorbance change ($\%A\ change = 100 \times (A(T) - A^\circ)/(A^\infty - A^\circ)$, where $A(T)$ is the absorbance read at each temperature $T$ (°C), $A^\circ$ the absorbance corresponding to the initial plateau and $A^\infty$ the absorbance for the final plateau), was plotted against temperature. In this way, a sigmoidal curve is obtained according to Eq. (1).

$$\%A\ change = \frac{A_T - A_0}{A_\infty - A_0} \times 100 \tag{1}$$

The melting temperature ($T_m$) was derived as the maximum of the first derivative of the sigmoidal curve. The concentration of the polynucleotide is around 20 μmol $dm^{-3}$ and the metal complex is put in an equal amount for the first experiment. If the stabilisation of the nucleotide is too high or too low, respectively lower or higher complex concentrations could be investigated. All the experiments were performed under the optimal ionic strength conditions so that the melting temperature of the polynucleotide alone is around 50–60 °C. These conditions allow the appreciation of possible enhancement of $T_m$.

#### 4.3.3. Viscosity

The viscometer used is a semi-micro type "Cannon-Ubbelohde" capillary viscometer. To carry out the measurement, 3.0 $cm^3$ of buffer solution (NaCl 0.1 mol $dm^{-3}$, NaCac 2.5 mmol $dm^{-3}$, pH = 7.0) volume was taken with a glass pipette and inserted into the viscosimeter in the lower tank. The viscometer was placed in a water bath at a constant temperature of 25.0 ± 0.1 °C and left to rest for 15 min to allow the solution to reach the desired temperature. The solution was sucked up with a small rubber pump until the liquid almost reaches the exit. After that, DNA was added with a micro-syringe Hamilton connected to a Mitutoyo micrometric screw (the same as the spectroscopic titrations) to have a $c_{DNA}$ = 100 μmol $dm^{-3}$ and the solution is mixed by pushing up and down the liquid. Every addition of the tested compound was made in the same way as the addition of DNA, like a titration. The flow time is measured with a digital stopwatch which corresponds to the time that the meniscus of the liquid takes to pass from the two notches. The operation must be carried out for the solvent used (measuring $t_{solv}$), for the solvent + DNA ($t_{DNA}$) mixture and for different solvent + DNA + molecule mixtures ($t_{sample}$). All the measurements were repeated at least 5 times. After each use, a washing cycle must be carried out: water - acetone - water - ethanol - $N_2$.

The relative viscosity of the polynucleotide was calculated by Eq. (2):

$$\frac{\eta}{\eta_0} = \frac{t_{sample} - t_{solv}}{t_{DNA} - t_{solv}} \tag{2}$$

The relative viscosity is connected to the polynucleotide elongation by Eq. (3).

$$\frac{L}{L_0} = \left(\frac{\eta}{\eta_0}\right)^{\frac{1}{3}} \tag{3}$$

where $L$ is the length of the bound polynucleotide and $L_0$ is the length of the free one.

#### 4.3.4. pUC18 extraction

*E. coli* DH5α was cultured in 100 $cm^3$ of LB (Luria-Bertani) medium with 50 × $10^{-6}$ $dm^3$ of ampicillin overnight at 37.0 °C in IKA™ KS4000i Incubator Shakers. The next day extraction of plasmid DNA (pUC18) was performed following the protocol in OMEGA biotek plasmid DNA

kit. The absorbance ratio $A_{260nm}/A_{280nm} > 1.8$ was checked, to ensure the absence of significant protein amounts. The pUC18 concentration was measured by spectrophotometry as $c_{pUC18} = A_{260nm} \times 50$ μg cm$^{-3}$. Gel electrophoresis was done to also check that only the two bands of OC (open circular) and SC (supercoiled) forms do appear for pUC18 alone.

#### 4.3.5. Agarose gel electrophoresis

Agarose gel electrophoresis of pUC18 was performed after overnight incubation at 37.0 °C of the plasmid (6.5 μmol dm$^{-3}$, base pairs) in the presence of different increasing concentrations of the tested metal complex or cisplatin in buffer (NaCl 0.1 mol dm$^{-3}$, NaCac 2.5 mmol dm$^{-3}$, pH = 7.0). A vehicle-treated pUC18 sample was included with the maximum DMSO concentration used in the electrophoresis experiment. Loading buffer ($4 \times 10^{-6}$ dm$^3$) was added to each sample ($20 \times 10^{-6}$ dm$^3$) before being loaded onto 1 % agarose gel. Electrophoresis was run at 60 V for 2 h and 10 min. After the run, the gel was stained with a solution of ethidium bromide 1 μg cm$^{-3}$ in TAE 1× for 1 h. Finally, the gel was visualized by exposure to UV light (312 nm) by a Gel Doc XR + Imaging System (Bio-Rad). Another electrophoresis experiment was carried out in the same way, incubating the samples with ROS scavengers when cleavage of DNA was observed. L-histidine (L-His, for $^1O_2$), DMSO (for OH•), sodium pyruvate (pyr, for $H_2O_2$), and superoxide dismutase (SOD, for $O_2^-$) were used to detect which ROS was produced [39].

#### 4.3.6. Native gel electrophoresis

Native polyacrylamide gel electrophoresis (PAGE) tests were performed by incubating BSA (3 μmol dm$^{-3}$) overnight with different concentrations of metal complexes for [complex]/[protein] concentration ratios of 5, 10 and 20 in NaCl 0.1 mol dm$^{-3}$, NaCac 2.5 mmol dm$^{-3}$ buffer pH = 7.0 and $T$ = 37.0 °C. After that, $6 \times 10^{-6}$ dm$^3$ of sample buffer 2× (0.01 % bromophenol blue and 20 % glycerol in Tris HCl buffer 0.5 mol dm$^{-3}$, pH = 6.8) were added to $6 \times 10^{-6}$ dm$^3$ of the sample solutions (final $c_{BSA}$ = 1.5 μmol dm$^{-3}$) and loaded onto 10 % polyacrylamide gels. Before the loading of the samples, a pre-run was done at 200 V for 1 h, to remove any possible impurity from the gel. Gels were run in native PAGE buffer 250 mmol dm$^{-3}$ Tris Base, 1.92 mol dm$^{-3}$ glycine, pH = 8.3 at 80 V for 4 h at 4 °C to avoid denaturation of the protein. Finally, gels were stained with Coomassie Brilliant Blue R-250.

#### 4.3.7. $LogP_{o/w}$

The octanol-water partition coefficients were determined as follows. Water (500 cm$^3$, distilled after MilliQ purification) and n-octanol (500 cm$^3$) were shaken together for 72 h to allow saturation of both phases (one week for the full separation of the two phases). Approximately 0.5 mg of the complexes were placed into a Falcon tube, and 2.0 cm$^3$ of octanol-saturated water and 2.0 cm$^3$ of water-saturated octanol were added into the same Falcon of the compound and shacked until the complexes were fully dissolved and divided into the two phases. Biphasic solutions were mixed for ten minutes and then centrifuged for five minutes at 6000 rpm to allow separation. Two aliquots of 0.50 cm$^3$ for both phases were placed into metal-free PE tubes and 4.0 cm$^3$ of 3HCl: $HNO_3$ (*aqua regia*) solution Suprapure (dilution 1:1 with MilliQ water) were added to the aliquots to obtain 4 samples for each complex (2 for the water phase and 2 for the octanol phase). The solutions were mineralised at 90 °C overnight and 1.5 cm$^3$ of MilliQ water were added at the end to have a final volume of 6.0 cm$^3$ for each sample. Concentrations of both phases were determined by ICP-OES.

Reported $logP_{o/w}$ is defined as in Eq. (4):

$$logP_{o/w} = log\frac{[complex]_o}{[complex]_w} \quad (4)$$

Final values were reported as the mean of two determinations.

#### 4.3.8. Cell culture

A549 (lung adenocarcinoma) and SW480 (colon adenocarcinoma) cells were cultured in Dulbecco's Modified Eagle's Medium (DMEM), whereas A2780 (ovarian carcinoma) and A2789cis (ovarian carcinoma cisplatin-resistant) cells in Roswell Park Memorial Institute (RPMI) 1640 medium supplemented with 2 mmol dm$^{-3}$ L-glutamine, and HEK293 (embryonic kidney) cells in Eagle's Minimum Essential Medium (EMEM) supplemented with 1 % of non-essential amino acids. All media were supplemented with 10 % fetal bovine serum (FBS), fundamental for cell growth, and 1 % amphotericin-penicillin-streptomycin solution (all from Sigma Aldrich). The antibiotic is added to prevent bacterial contamination. Cell cultures are grown in a plastic flask in 10 cm$^3$ of cell culture media and incubated in a humid atmosphere at 37 °C under a 5 % $CO_2$ atmosphere. Once 90 % of confluence is reached, subculture is performed by trypsinization. The cells are resuspended in 1.0 cm$^3$ of PBS and counted to have the desired cell concentration.

#### 4.3.9. MTT-assay – antiproliferative activity

Approximately $5 \times 10^3$ A549, $1 \times 10^4$ SW480, $2 \times 10^4$ A2780, A2780cis and HEK293 cells per well were seeded in 0.200 cm$^3$ of their culture medium in 96-well plates and incubated for 24 h at 37 °C under a 5 % $CO_2$ atmosphere. Then, the cells were treated with different concentrations of the complexes under study for 24 h. Cisplatin (CDDP) was used as a positive control at its $IC_{50}$ value (4 wells), and the max percentage of DMSO as a negative control (4 wells). 8 wells were seeded without treatment to have the maximum value for alive cells. Afterwards, the medium was removed, and cells were incubated with 0.100 cm$^3$ of MTT (3-(4,5-dimethyltiazol-2-yl)-2,5-diphenyltetrazolium-bromide) (Sigma Aldrich) dissolved in culture medium (500 mg cm$^{-3}$). The reduction of the yellow salt, thanks to mitochondrial dehydrogenase, forms the blue formazan in the living cells. After 3–4 h of incubation, the formazan crystals were dissolved by overnight incubation with 0.100 cm$^3$ of the solubilized solution (10 % SDS and 0.01 mol dm$^{-3}$ HCl). Finally, the absorbance was read at 590 nm on a microplate reader (Cytation 5 Cell Imaging Multi-Mode ReaderBiotek Instruments, USA). Four replicates per dose were included and at least two independent experiments were performed for the calculation of the half-maximal inhibitory concentration ($IC_{50}$) values employing GraphPadPrism Software Inc. (version 6.01) (USA).

#### 4.3.10. Flow cytometry

Apoptosis was evaluated by flow cytometry with an Annexin V:FITC Assay Kit (Biorad) according to the manufacturer's instructions. $2 \times 10^5$ SW480 cells were seeded in 1.0 cm$^3$ of cell culture medium in 12 well plates. After 24 h of incubation, the cells were treated with the half-maximal inhibitory concentration of each complex for 24 h. Cisplatin (CDDP) was used as positive apoptotic control, while TRITON 1 % was used as death (necrotic) control and added 10 min before the harvesting of the cells. Afterwards, the cells were washed with cold PBS, harvested, and resuspended in a binding buffer. Then, the cells were doubly stained with the Annexin V:FITC conjugate and propidium iodide (PI). Immediately after PI addition, the cells were injected in a NovoCyte Flow cytometer (ACEA Biosciences, Inc., USA). 10,000 events were counted and analysed by using the NovoExpress 1.4.0 Software. Two replicates and two independent experiments were performed.

#### 4.3.11. Cell uptake

$1.5 \times 10^5$ SW480 cells were seeded in 2.0 cm$^3$ of cell culture medium in 6 well plates for 24 h. Afterwards, the cells were treated with a concentration of 5 μmol dm$^{-3}$ for each metal complex for 24 h. CDDP was used as a positive and reference control. Afterwards, the cells were harvested and then washed twice with PBS to remove the metal complex that was not internalised to obtain the cell pellet. The cells were counted by resuspending them in 0.500 cm$^3$ of PBS to obtain the cell concentration (number of cells cm$^{-3}$). 2.0 cm$^3$ of HCl/$HNO_3$ 3:1 mixture (*aqua regia*) Suprapure solution (dilution 1:1 with MilliQ water) were added to

mineralise the samples (90 °C overnight). A dilution with MilliQ water to have a final volume of 6.0 $cm^3$ per sample was done, and an ICP-OES analysis was performed to have the concentration of each metal centre internalised by the cells expressed in μg of metal/number of cells.

## CRediT authorship contribution statement

**Francesca Binacchi:** Writing – original draft, Methodology, Investigation, Formal analysis. **Damiano Cirri:** Writing – review & editing, Methodology, Investigation. **Eleonora Bimbi:** Investigation, Formal analysis. **Natalia Busto:** Writing – review & editing, Supervision, Resources, Project administration, Methodology, Funding acquisition, Conceptualization. **Alessandro Pratesi:** Writing – review & editing, Supervision, Resources, Project administration, Methodology, Funding acquisition, Conceptualization. **Tarita Biver:** Writing – review & editing, Supervision, Resources, Project administration, Methodology, Funding acquisition, Conceptualization.

## Declaration of competing interest

The authors declare that they have no known competing financial interests or personal relationships that could have appeared to influence the work reported in this paper.

## Data availability

Data will be made available on request.

## Acknowledgements

This contribution is part of the work from COST Action CA18202, NECTAR Network for Equilibria and Chemical Thermodynamics Advanced Research, supported by COST (European Cooperation in Science and Technology).

NB acknowledges Ministerio de Ciencia e Innovación of Spain (PID2022-142318NB-I00) for financial support.

AP gratefully acknowledges funding by the University of Pisa under the "PRA–Progetti di Ricerca di Ateneo" (Institutional Research Grants), project no. PRA_2022–2023_12 "New challenges of transition metal and lanthanide complexes in the perspective of green chemistry". The CIRCC (Interuniversity Consortium for Chemical Reactivity and Catalysis) is also acknowledged.

## Appendix A. Supplementary data

Supplementary data to this article can be found online at https://doi.org/10.1016/j.jinorgbio.2024.112749.

## References

[1] E. Giorgi, F. Binacchi, C. Marotta, D. Cirri, C. Gabbiani, A. Pratesi, Highlights of new strategies to increase the efficacy of transition metal complexes for Cancer treatments, Molecules 28 (2022) 273, https://doi.org/10.3390/molecules28010273.

[2] S. Medici, M. Peana, V.M. Nurchi, J.I. Lachowicz, G. Crisponi, M.A. Zoroddu, Noble metals in medicine: latest advances, Coord. Chem. Rev. 284 (2015) 329–350, https://doi.org/10.1016/j.ccr.2014.08.002.

[3] F.H. Abdalbari, C.M. Telleria, The gold complex auranofin: new perspectives for cancer therapy, Discov. Oncol. 12 (2021) 42, https://doi.org/10.1007/s12672-021-00439-0.

[4] S.M. Meier-Menches, C. Gerner, W. Berger, C.G. Hartinger, B.K. Keppler, Structure–activity relationships for ruthenium and osmium anticancer agents – towards clinical development, Chem. Soc. Rev. 47 (2018) 909–928, https://doi.org/10.1039/C7CS00332C.

[5] T.J. Carneiro, A.S. Martins, M.P.M. Marques, A.M. Gil, Metabolic aspects of palladium(II) potential anti-Cancer drugs, Front. Oncol. 10 (2020) 590970, https://doi.org/10.3389/fonc.2020.590970.

[6] N.J. Patel, B.S. Bhatt, M.N. Patel, Heteroleptic N,N-donor pyrazole based Pt(II) and Pd(II) complexes: DNA binding, molecular docking and cytotoxicity studies, Inorg. Chim. Acta 498 (2019) 119130, https://doi.org/10.1016/j.ica.2019.119130.

[7] E.-J. Gao, S.-M. Zhao, D. Zhang, Q.-T. Liu, Study on the interaction of ternary complex Pd(II)-2,2?-bipyridine-L-asparagic acid with DNA, Chin. J. Chem. 23 (2005) 54–57, https://doi.org/10.1002/cjoc.200590012.

[8] E.-J. Gao, K.-H. Wang, X.-F. Gu, Y. Yu, Y.-G. Sun, W.-Z. Zhang, H.-X. Yin, Q. Wu, M.-C. Zhu, X.-M. Yan, A novel binuclear palladium complex with benzothiazole-2-thiolate: synthesis, crystal structure and interaction with DNA, J. Inorg. Biochem. 101 (2007) 1404–1409, https://doi.org/10.1016/j.jinorgbio.2007.06.007.

[9] A.S. Abu-Surrah, H.H. Al-Sa'doni, M.Y. Abdalla, Palladium-based chemotherapeutic agents: routes toward complexes with good antitumor activity, Cancer Ther. 6 (2008) 1–10.

[10] M. Feizi-Dehnayebi, E. Dehghanian, H. Mansouri-Torshizi, DNA/BSA binding affinity studies of new Pd(II) complex with S-S and N-N donor mixed ligands via experimental insight and molecular simulation: preliminary antitumor activity, lipophilicity and DFT perspective, J. Mol. Liq. 344 (2021) 117853, https://doi.org/10.1016/j.molliq.2021.117853.

[11] M. Gasperini, Carbonylation of nitrobenzene to N-methyl phenylcarbamate catalyzed by palladium–phenanthroline complexes bifunctional activation by anthranilic acid, J. Mol. Catal. A Chem. 204–205 (2003) 107–114, https://doi.org/10.1016/S1381-1169(03)00289-9.

[12] F. Ragaini, M. Gasperini, S. Cenini, L. Arnera, A. Caselli, P. Macchi, N. Casati, Mechanistic study of the palladium–phenanthroline catalyzed carbonylation of nitroarenes and amines: palladium–carbonyl intermediates and bifunctional effects, Chem. Eur. J. 15 (2009) 8064–8077, https://doi.org/10.1002/chem.200801882.

[13] V.X. Jin, J.D. Ranford, Complexes of platinum(II) or palladium(II) with 1,10-phenanthroline and amino acids, Inorg. Chim. Acta 304 (2000) 38–44, https://doi.org/10.1016/S0020-1693(00)00061-X.

[14] C.V. Barra, F.V. Rocha, L. Morel, A. Gautier, S.S. Garrido, A.E. Mauro, R.C.G. Frem, A.V.G. Netto, DNA binding, topoisomerase inhibition and cytotoxicity of palladium (II) complexes with 1,10-phenanthroline and thioureas, Inorg. Chim. Acta 446 (2016) 54–60, https://doi.org/10.1016/j.ica.2016.02.053.

[15] A. Gil, M. Melle-Franco, V. Branchadell, M.J. Calhorda, How the intercalation of phenanthroline affects the structure, energetics, and bond properties of DNA base pairs: theoretical study applied to adenine–thymine and guanine–cytosine tetramers, J. Chem. Theory Comput. 11 (2015) 2714–2728, https://doi.org/10.1021/ct5006104.

[16] D. Ajloo, M. Eslami Moghadam, K. Ghadimi, M. Ghadamgahi, A.A. Saboury, A. Divsalar, M. SheikhMohammadi, K. Yousefi, Synthesis, characterization, spectroscopy, cytotoxic activity and molecular dynamic study on the interaction of three palladium complexes of phenanthroline and glycine derivatives with calf thymus DNA, Inorg. Chim. Acta 430 (2015) 144–160, https://doi.org/10.1016/j.ica.2015.03.006.

[17] J. Valladolid, C. Hortigüela, N. Busto, G. Espino, A.M. Rodríguez, J.M. Leal, F. A. Jalón, B.R. Manzano, A. Carbayo, B. García, Phenanthroline ligands are biologically more active than their corresponding ruthenium ( II ) arene complexes, Dalton Trans. 43 (2014) 2629–2645, https://doi.org/10.1039/C3DT52743C.

[18] T. Lazarević, A. Rilak, Ž.D. Bugarčić, Platinum, palladium, gold and ruthenium complexes as anticancer agents: current clinical uses, cytotoxicity studies and future perspectives, Eur. J. Med. Chem. 142 (2017) 8–31, https://doi.org/10.1016/j.ejmech.2017.04.007.

[19] B.B. Zmejkovski, N.Đ. Pantelić, G.N. Kaluđerović, Palladium(II) complexes: structure, development and cytotoxicity from cisplatin analogues to chelating ligands with N stereocenters, Inorg. Chim. Acta 534 (2022) 120797, https://doi.org/10.1016/j.ica.2022.120797.

[20] D.I. Ugwu, J. Conradie, Anticancer properties of complexes derived from bidentate ligands, J. Inorg. Biochem. 246 (2023) 112268, https://doi.org/10.1016/j.jinorgbio.2023.112268.

[21] A. Abu-Surrah, M. Kettunen, Platinum group antitumor chemistry: design and development of new anticancer drugs complementary to cisplatin, Curr. Med. Chem. 13 (2006) 1337–1357, https://doi.org/10.2174/092986706776872970.

[22] M.I. Acuña, A.R. Rubio, M. Martínez-Alonso, N. Busto, A.M. Rodríguez, N. Davila-Ferreira, C. Smythe, G. Espino, B. García, F. Domínguez, Targets, mechanisms and cytotoxicity of half-Sandwich Ir(III) complexes are modulated by structural modifications on the Benzazole ancillary ligand, Cancers 15 (2022) 107, https://doi.org/10.3390/cancers15010107.

[23] J. Bogojeski, J. Volbeda, M. Freytag, M. Tamm, Ž.D. Bugarčić, Palladium( II ) complexes with highly basic imidazolin-2-imines and their reactivity toward small bio-molecules, Dalton Trans. 44 (2015) 17346–17359, https://doi.org/10.1039/C5DT02307F.

[24] S. Jovanović, K. Obrenčević, Ž.D. Bugarčić, I. Popović, J. Žakula, B. Petrović, New bimetallic palladium( II ) and platinum( II ) complexes: studies of the nucleophilic substitution reactions, interactions with CT-DNA, bovine serum albumin and cytotoxic activity, Dalton Trans. 45 (2016) 12444–12457, https://doi.org/10.1039/C6DT02226J.

[25] A. Schmidt, R. Guha, A. Hepp, J. Müller, Platinum(II) and palladium(II) complexes of tridentate hydrazone-based ligands as selective guanine quadruplex binders, J. Inorg. Biochem. 175 (2017) 58–66, https://doi.org/10.1016/j.jinorgbio.2017.07.003.

[26] O. Jarjayes, T. Lavergne, F. Thomas, Interaction of metal complexes with G-Quadruplexes, in: R.A. Scott (Ed.), Encycl. Inorg. Bioinorg. Chem, 2nd ed, Wiley, 2020, pp. 1–24, https://doi.org/10.1002/9781119951438.eibc2748.

[27] T. Biver, Discriminating between parallel, anti-parallel and hybrid G-quadruplexes: mechanistic details on their binding to small molecules, Molecules 27 (2022) 4165, https://doi.org/10.3390/molecules27134165.

[28] A. Łęczkowska, J. Gonzalez-Garcia, C. Perez-Arnaiz, B. Garcia, A.J.P. White, R. Vilar, Binding studies of metal–salphen and metal–bipyridine complexes

towards G-quadruplex DNA, Chem. Eur. J. 24 (2018) 11785–11794, https://doi.org/10.1002/chem.201802248.
[29] F. Binacchi, C. Elia, D. Cirri, C. Van de Griend, X.-Q. Zhou, L. Messori, S. Bonnet, A. Pratesi, T. Biver, A biophysical study of the interactions of palladium( II ), platinum( II ) and gold( III ) complexes of aminopyridyl-2,2′-bipyridine ligands with RNAs and other nucleic acid structures, Dalton Trans. (2023), https://doi.org/10.1039/D2DT03483B.
[30] X. Chen, M.-Y. Tsai, P.G. Wolynes, The role of charge density coupled DNA bending in transcription factor sequence binding specificity: a generic mechanism for indirect readout, J. Am. Chem. Soc. 144 (2022) 1835–1845, https://doi.org/10.1021/jacs.1c11911.
[31] F. Guarra, N. Busto, A. Guerri, L. Marchetti, T. Marzo, B. García, T. Biver, C. Gabbiani, Cytotoxic ag(I) and au(I) NHC-carbenes bind DNA and show TrxR inhibition, J. Inorg. Biochem. 205 (2020) 110998, https://doi.org/10.1016/j.jinorgbio.2020.110998.
[32] G. Marverti, G. Gozzi, A. Lauriola, G. Ponterini, S. Belluti, C. Imbriano, M.P. Costi, D. D'Arca, The 1,10-Phenanthroline ligand enhances the Antiproliferative activity of DNA-intercalating Thiourea-Pd(II) and -Pt(II) complexes against cisplatin-sensitive and -resistant human ovarian Cancer cell lines, Int. J. Mol. Sci. 20 (2019) 6122, https://doi.org/10.3390/ijms20246122.
[33] A. Kellett, Z. Molphy, C. Slator, V. McKee, N.P. Farrell, Molecular methods for assessment of non-covalent metallodrug–DNA interactions, Chem. Soc. Rev. 48 (2019) 971–988, https://doi.org/10.1039/C8CS00157J.
[34] N. Kumar, R. Kaushal, P. Awasthi, Non-covalent binding studies of transition metal complexes with DNA: a review, J. Mol. Struct. 1288 (2023) 135751, https://doi.org/10.1016/j.molstruc.2023.135751.
[35] S. Ramakrishnan, M. Palaniandavar, Mixed-ligand copper(II) complexes of dipicolylamine and 1,10-phenanthrolines: the role of diimines in the interaction of the complexes with DNA, J. Chem. Sci. 117 (2005) 179–186, https://doi.org/10.1007/BF03356114.
[36] M.R. Beccia, T. Biver, A. Pardini, J. Spinelli, F. Secco, M. Venturini, N. Busto Vázquez, M.P. Lopez Cornejo, V.I. Martin Herrera, R. Prado Gotor, The fluorophore 4′,6-Diamidino-2-phenylindole (DAPI) induces DNA folding in Long double-stranded DNA, Chem. Asian J. 7 (2012) 1803–1810, https://doi.org/10.1002/asia.201200177.
[37] T. Hidalgo, D. Fabra, R. Allende, A.I. Matesanz, P. Horcajada, T. Biver, A. G. Quiroga, Two novel Pd thiosemicarbazone complexes as efficient and selective antitumoral drugs, Inorg. Chem. Front. 10 (2023) 1986–1998, https://doi.org/10.1039/D2QI02424A.
[38] N. Busto, M. Martínez-Alonso, J.M. Leal, A.M. Rodríguez, F. Domínguez, M. I. Acuña, G. Espino, B. García, Monomer–dimer divergent behavior toward DNA in a half-sandwich ruthenium(II) aqua complex. Antiproliferative biphasic activity, Organometallics 34 (2015) 319–327, https://doi.org/10.1021/om5011275.
[39] A.R. Rubio, R. González, N. Busto, M. Vaquero, A.L. Iglesias, F.A. Jalón, G. Espino, A.M. Rodríguez, B. García, B.R. Manzano, Anticancer activity of half-Sandwich Ru, Rh and Ir complexes with chrysin derived ligands: strong effect of the side chain in the ligand and influence of the metal, Pharmaceutics 13 (2021) 1540, https://doi.org/10.3390/pharmaceutics13101540.
[40] M. Muralisankar, S.M. Basheer, J. Haribabu, N.S.P. Bhuvanesh, R. Karvembu, A. Sreekanth, An investigation on the DNA/protein binding, DNA cleavage and *in vitro* anticancer properties of SNO pincer type palladium(II) complexes with N-substituted isatin thiosemicarbazone ligands, Inorg. Chim. Acta 466 (2017) 61–70, https://doi.org/10.1016/j.ica.2017.05.044.
[41] C. Icsel, V.T. Yilmaz, DNA binding and cleavage studies of two palladium(II) Saccharinate complexes with Terpyridine, DNA Cell Biol. 32 (2013) 165–172, https://doi.org/10.1089/dna.2012.1959.
[42] M.S. Ragab, M.R. Shehata, M.M. Shoukry, M. Haukka, M.A. Ragheb, Oxidative DNA cleavage mediated by a new unexpected [Pd(BAPP)][$PdCl_4$] complex (BAPP = 1,4-bis(3-aminopropyl)piperazine): crystal structure. DNA binding and cytotoxic behavior, RSC Adv. 12 (2022) 1871–1884, https://doi.org/10.1039/D1RA07793G.
[43] K. Karami, N. Jamshidian, M. Zakariazadeh, A.A. Momtazi-Borojeni, E. Abdollahi, Z. Amirghofran, A. Shahpiri, A.K. Nasab, Experimental and theoretical studies of palladium-hydrazide complexes' interaction with DNA and BSA, *in vitro* cytotoxicity activity and plasmid cleavage ability, Comput. Biol. Chem. 91 (2021) 107435, https://doi.org/10.1016/j.compbiolchem.2021.107435.
[44] T. Biver, F. Secco, M. Venturini, Mechanistic aspects of the interaction of intercalating metal complexes with nucleic acids, Coord. Chem. Rev. 252 (2008) 1163–1177, https://doi.org/10.1016/j.ccr.2007.10.008.
[45] V. Anbalagan, T.S. Srivastava, Spectral and photochemical behaviour of mononuclear and dinuclear α-diimine complexes of Pt(II) and Pd(II) with catechol derivatives, J. Photochem. Photobiol. A Chem. 89 (1995) 113–119, https://doi.org/10.1016/1010-6030(94)04005-M.
[46] C. Pérez-Arnaiz, J. Leal, N. Busto, M.C. Carrión, A.R. Rubio, I. Ortiz, G. Barone, B. Díaz De Greñu, J. Santolaya, J.M. Leal, M. Vaquero, F.A. Jalón, B.R. Manzano, B. García, Role of Seroalbumin in the cytotoxicity of *cis*- Dichloro Pt(II) complexes with (N^N)-donor ligands bearing functionalized tails, Inorg. Chem. 57 (2018) 6124–6134, https://doi.org/10.1021/acs.inorgchem.8b00713.
[47] G. Felsenfeld, S.Z. Hirschman, A neighbor-interaction analysis of the hypochromism and spectra of DNA, J. Mol. Biol. 13 (1965) 407–427, https://doi.org/10.1016/S0022-2836(65)80106-1.
[48] X. Long, M.D. Stone, Kinetic partitioning modulates human telomere DNA G-Quadruplex structural polymorphism, PLoS ONE 8 (2013) e83420, https://doi.org/10.1371/journal.pone.0083420.
[49] T. Biver, F. Secco, M. Venturini, Relaxation kinetics of the interaction between RNA and metal-intercalators: the poly(a)·poly(U)/platinum-proflavine system, Arch. Biochem. Biophys. 437 (2005) 215–223, https://doi.org/10.1016/j.abb.2005.03.009.
[50] F.J. Hoyuelos, B. García, J.M. Leal, N. Busto, T. Biver, F. Secco, M. Venturini, RNA triplex-to-duplex and duplex-to-triplex conversion induced by coralyne, Phys. Chem. Chem. Phys. 16 (2014) 6012, https://doi.org/10.1039/c3cp52270a.
[51] A.R. Rubio, N. Busto, J.M. Leal, B. García, Doxorubicin binds to duplex RNA with higher affinity than ctDNA and favours the isothermal denaturation of triplex RNA, RSC Adv. 6 (2016) 101142–101152, https://doi.org/10.1039/C6RA21387A.
[52] H. Mach, C.R. Middaugh, R.V. Lewis, Statistical determination of the average values of the extinction coefficients of tryptophan and tyrosine in native proteins, Anal. Biochem. 200 (1992) 74–80, https://doi.org/10.1016/0003-2697(92)90279-G.